

Supporting Information for

## **Biogeochemical properties and transports in the North East Atlantic**

Clare Johnson<sup>1</sup>, Neil Fraser<sup>1</sup>, Stuart Cunningham<sup>1</sup>, Kristin Burmeister<sup>1</sup>, Sam Jones<sup>1</sup>, Lewis Drysdale<sup>1</sup>, Richard Abell<sup>1</sup>, Peter Brown<sup>2</sup>, Estelle Dumont<sup>1</sup>, Alan Fox<sup>1</sup>, N. Penny Holliday<sup>2</sup>, Mark Inall<sup>1</sup> and Sarah Reed<sup>1,3</sup>

<sup>1</sup>Scottish Association for Marine Science, Oban, Argyll, Scotland, PA37 1QA. <sup>2</sup>National Oceanography Centre, European Way, Southampton, UK, SO14 3ZH. <sup>3</sup>Current address: SEN Transmission, SSE, Henderson Road, Inverness, IV1 1SN.

### **Contents of this file**

Figures S1-S10  
Tables S1-S6

### **Introduction**

This supplementary information contains:

(1) figures and tables related to the performance of the Predictive Regression Equations (PREs) used to derive nutrient and carbon concentrations (Figures S1-7, Tables S1-5). See sections 3.1 and 3.2 in the main manuscript for full details of the methodology.

(2) details of the errors associated with the calculation of nutrient and carbon transports through the Rockall Trough (Table S6). See sections 3.3. and 3.4 in the main manuscript for full details of the methodology.

(3) figures evaluating the seasonal cycles for derived nutrients at several depths (Figures S8-10). See section 4.4 in the main manuscript for more details.

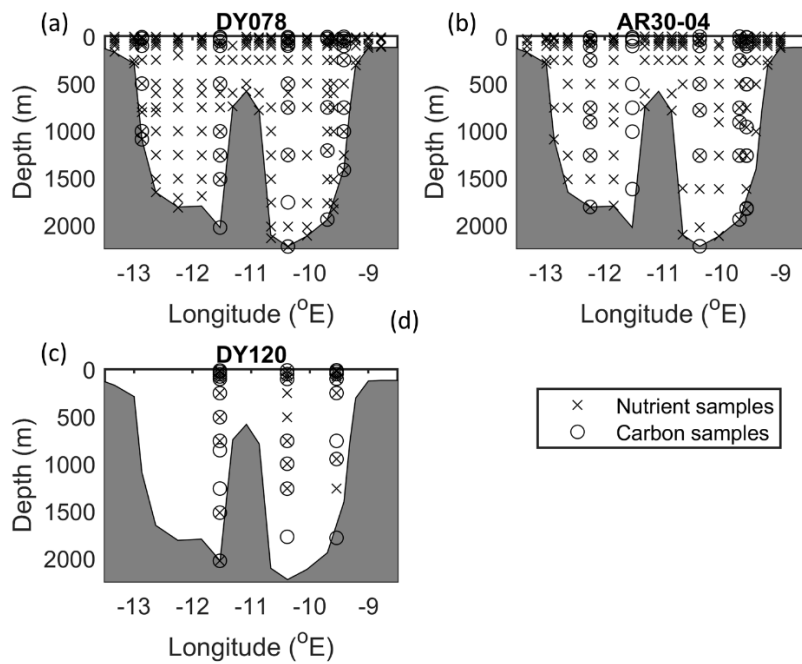


**Figure S1.** Location of water samples taken during the annual-biannual hydrographic sections, (a) DY078, (b) AR30-04, (c) DY120. Crosses show samples collected for the analysis of dissolved inorganic nutrients, and circles samples analysed for dissolved inorganic carbon and total alkalinity.

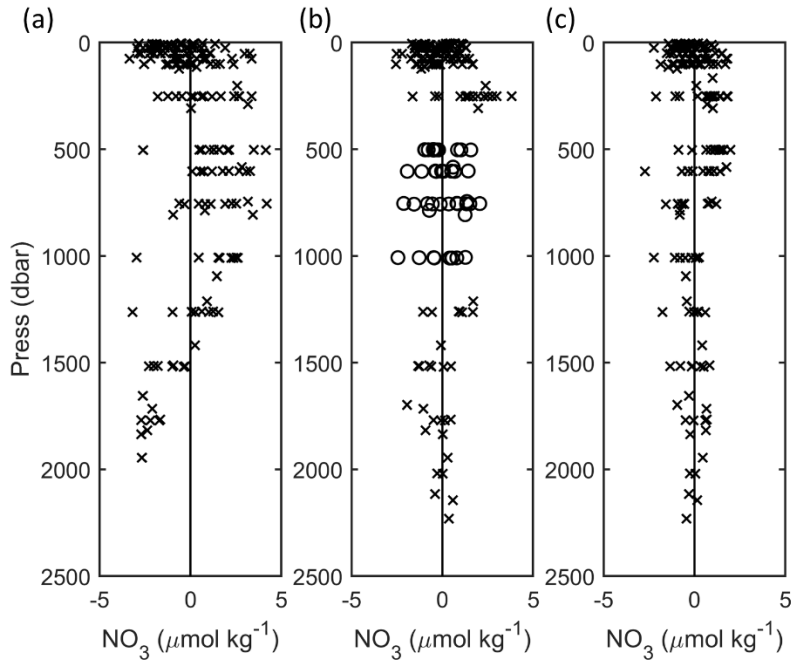


**Figure S2.** Profiles of residuals associated with the 2017 PREs for nitrate. (a) PRE using a predictor matrix of  $\theta$ , SP, P for the whole water column. (b) PREs using a predictor matrix of  $\theta$ , SP, P for areas outside the oxygen minimum layer (crosses) and within the lower oxygen layer (circles). (c) PRE using a predictor matrix of  $\theta$ , SP, P, DO for the whole water column. Similar results are seen for phosphate and silicate.

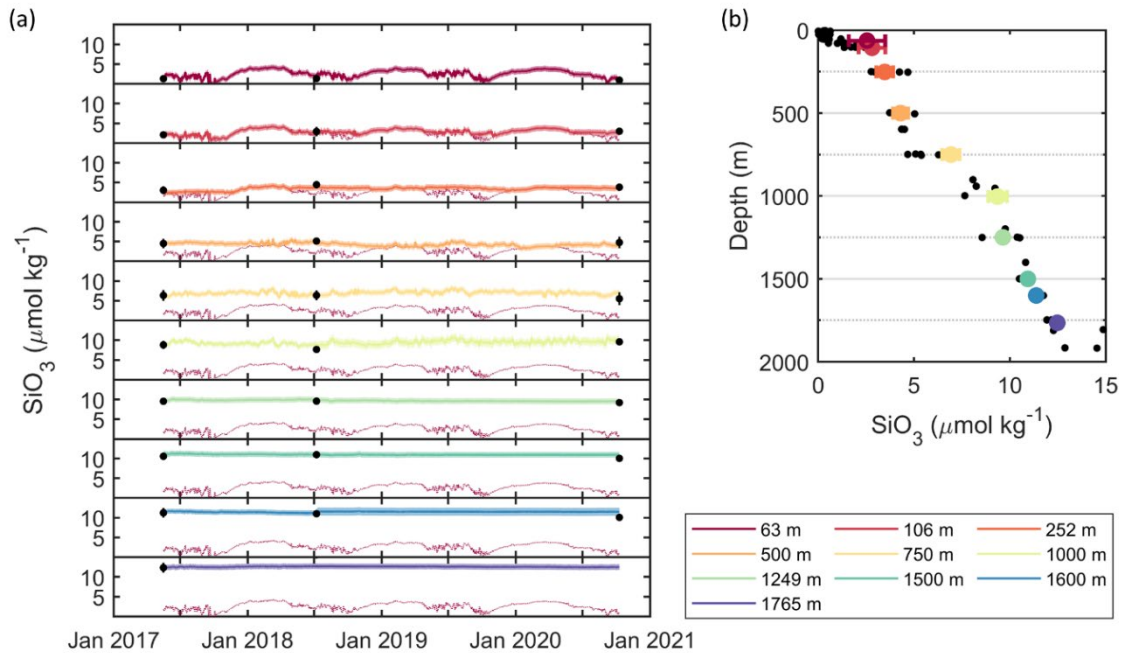


**Figure S3.** Derived silicate concentrations at different depths on mooring EB1 (colors) compared to lowered rosette data from the annual-biannual hydrographic cruises (black circles). On (a) the shaded envelope shows the RMSE associated with the PEs (Tables S1-S4) and the filled black circles the mean of any hydrographic data collected within 50 m of the mean moored instrument depth (125 m for instruments deeper than 1500 m). The derived timeseries from 63 dbar is shown as a thin line on all subplots. On (b), colored circles show the mean derived concentration and the error bars  $\pm$  one standard deviation, and black circles hydrographic data from the three stations closest to EB1 during the 2017, 2018 and 2020 hydrographic sections.

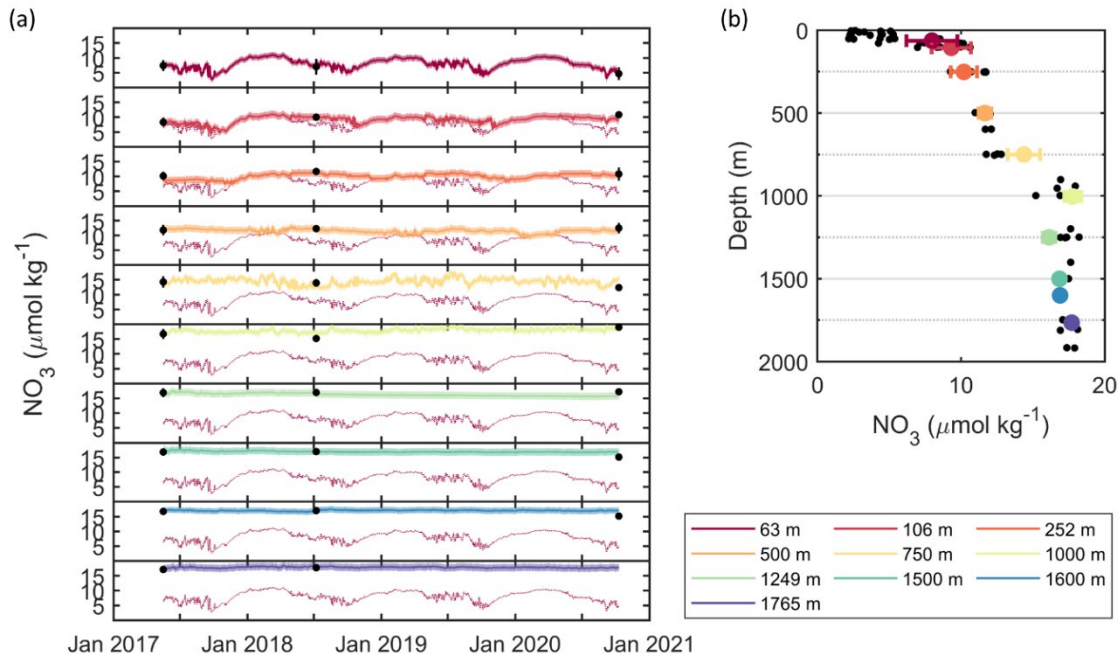


**Figure S4.** Derived nitrate concentrations at different depths on mooring EB1 (colors) compared to lowered rosette data from the annual-biannual hydrographic cruises (black circles). On (a) the shaded envelope shows the RMSE associated with the PReS (Tables S1-S4) and the filled black circles the mean of any hydrographic data collected within 50 m of the mean moored instrument depth (125 m for instruments deeper than 1500 m). The derived timeseries from 63 dbar is shown as a thin line on all subplots. On (b), colored circles show the mean derived concentration and the error bars  $\pm$  one standard deviation, and black circles hydrographic data from the three stations closest to EB1 during the 2017, 2018 and 2020 hydrographic sections.

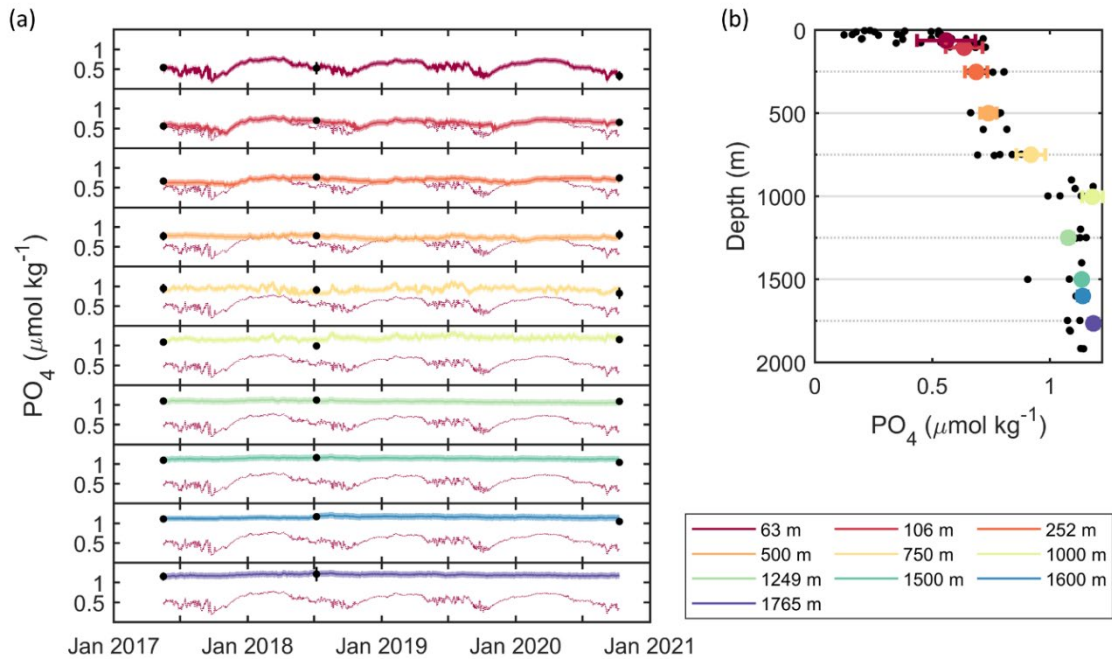


**Figure S5.** Derived phosphate concentrations at different depths on mooring EB1 (colors) compared to lowered rosette data from the annual-biannual hydrographic cruises (black circles). On (a) the shaded envelope shows the RMSE associated with the PREs (Tables S1-S4) and the filled black circles the mean of any hydrographic data collected within 50 m of the mean moored instrument depth (125 m for instruments deeper than 1500 m). The derived timeseries from 63 dbar is shown as a thin line on all subplots. On (b), colored circles show the mean derived concentration and the error bars  $\pm$  one standard deviation, and black circles hydrographic data from the three stations closest to EB1 during the 2017, 2018 and 2020 hydrographic sections.

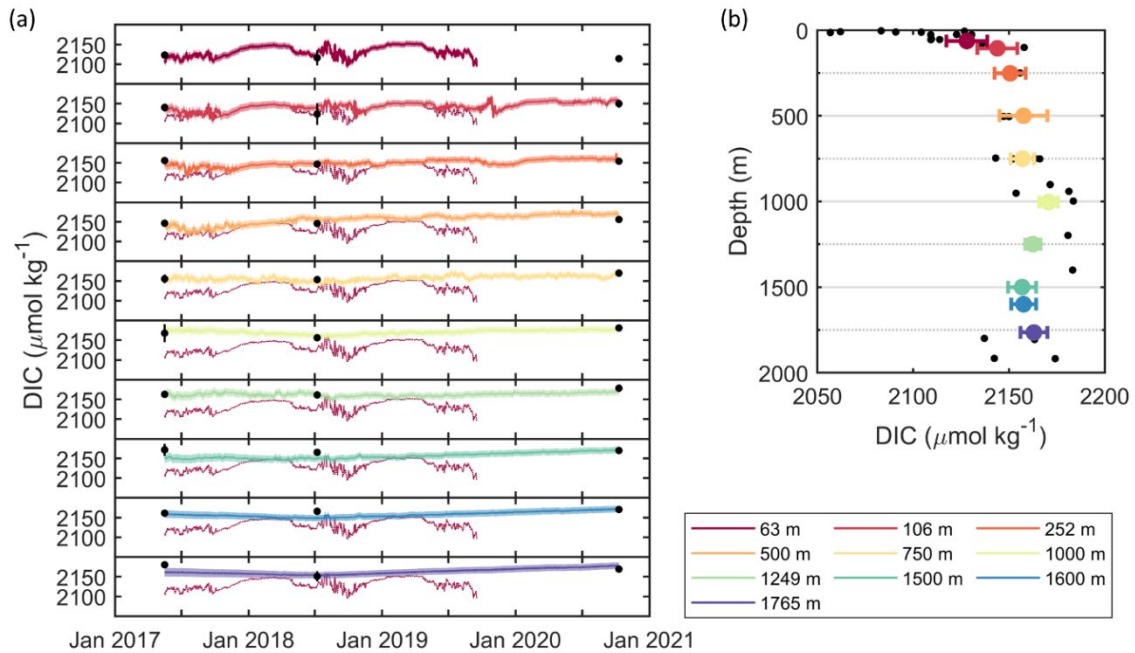


**Figure S6.** Derived dissolved inorganic carbon (DIC) levels at different depths on mooring EB1 (colors) compared to lowered rosette data from the annual-biannual hydrographic cruises (black circles). On (a) the shaded envelope shows the RMSE associated with the PREs (Tables S1-S4) and the filled black circles the mean of any hydrographic data collected within 50 m of the mean moored instrument depth (125 m for instruments deeper than 1500 m). The derived timeseries from 63 dbar is shown as a thin line on all subplots. On (b), colored circles show the mean derived concentration and the error bars  $\pm$  one standard deviation, and black circles hydrographic data from the three stations closest to EB1 during the 2017, 2018 and 2020 hydrographic sections.

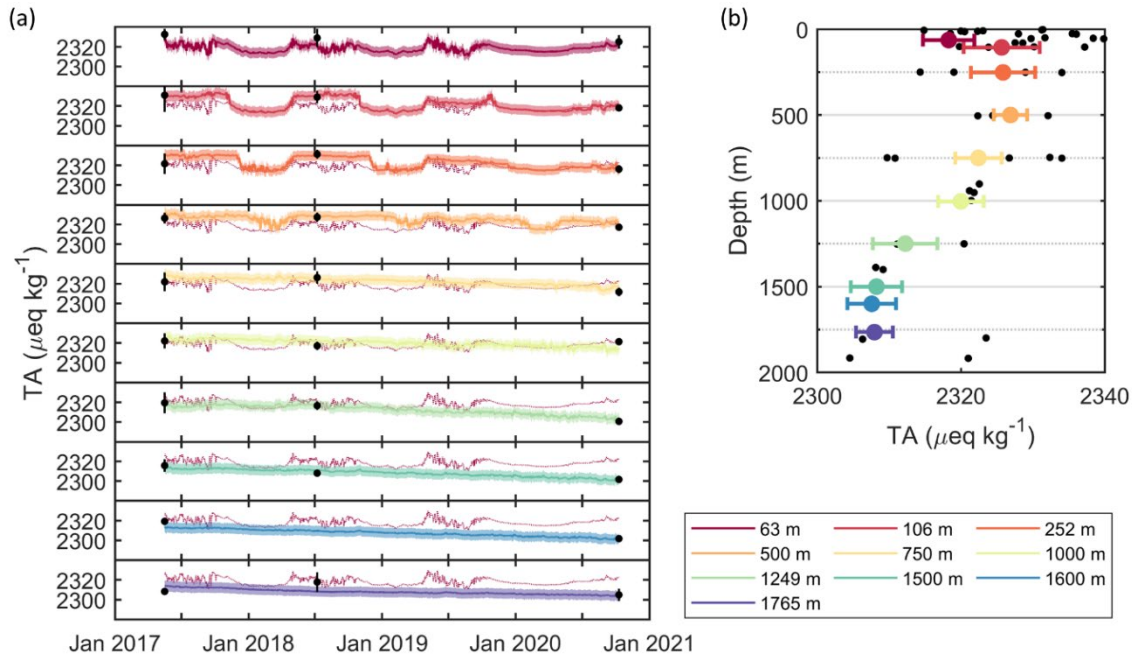


**Figure S7.** Derived total alkalinity (TA) levels at different depths on mooring EB1 (colors) compared to lowered rosette data from the annual-biannual hydrographic cruises (black circles). On (a) the shaded envelope shows the RMSE associated with the PREs (Tables S1-S4) and the filled black circles the mean of any hydrographic data collected within 50 m of the mean moored instrument depth (125 m for instruments deeper than 1500 m). The derived timeseries from 63 dbar is shown as a thin line on all subplots. On (b), colored circles show the mean derived concentration and the error bars  $\pm$  one standard deviation, and black circles hydrographic data from the three stations closest to EB1 during the 2017, 2018 and 2020 hydrographic sections.



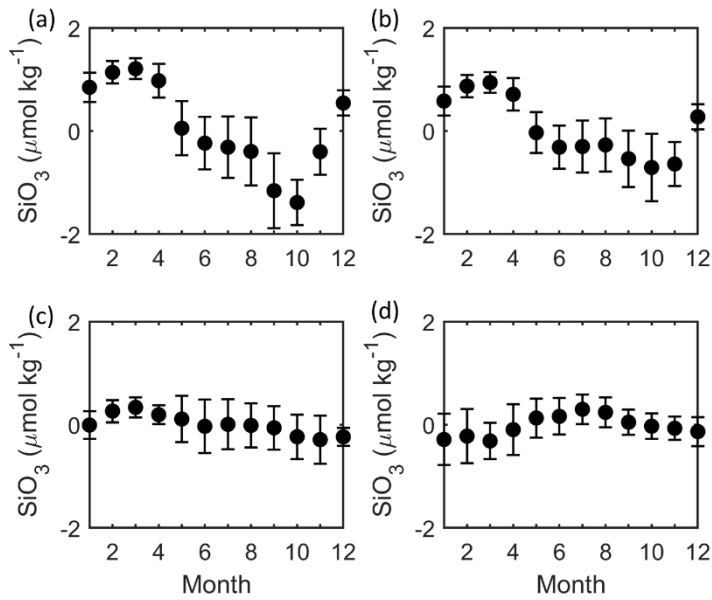


**Figure S8.** Monthly mean (circles)  $\pm$  1 standard deviation (error bars) of silicate anomalies relative to the mean at (a) 63 m, (b) 106 m, (c) 252 m, and (d) 500 m. Silicate values are derived from the PREs as described in section 3.

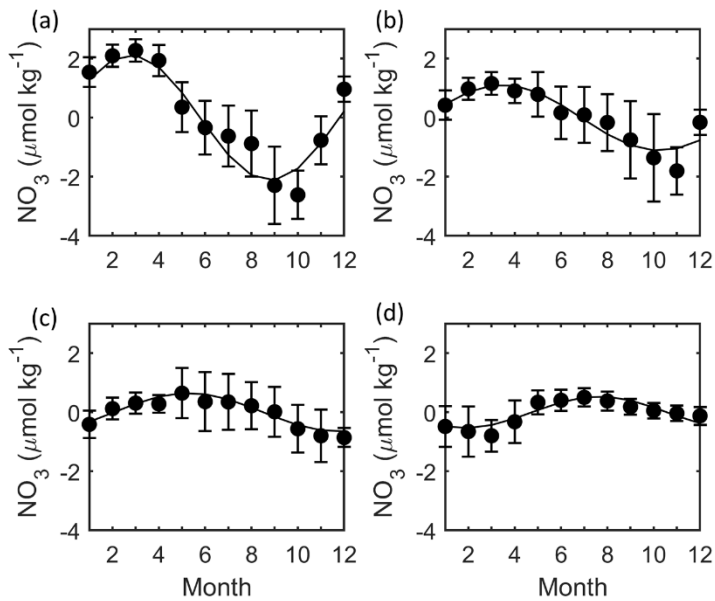


**Figure S9.** Monthly mean (circles)  $\pm$  1 standard deviation (error bars) of nitrate anomalies relative to the mean at (a) 63 m, (b) 106 m, (c) 252 m, and (d) 500 m. Nitrate values are derived from the PREs as described in section 3. The curves shown are used to correct Extended Ellett Line data to the annual mean in the calculation of nitrate transport during a weak subpolar gyre (see section 5).

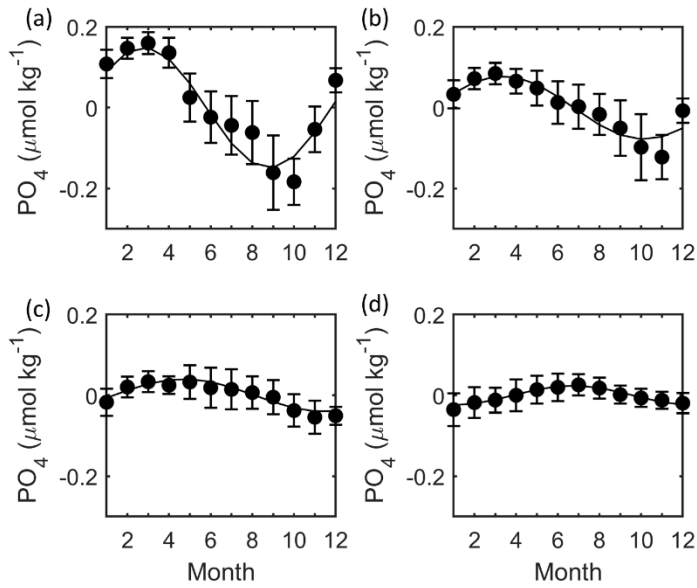


**Figure S10.** Monthly mean (circles)  $\pm$  1 standard deviation (error bars) of phosphate anomalies relative to the mean at (a) 63 m, (b) 106 m, (c) 252 m, and (d) 500 m. Phosphate values are derived from the PREs as described in section 3. The curves shown are used to correct Extended Ellett Line data to the annual mean in the calculation of phosphate transport during a weak subpolar gyre (see section 5).

		2017 Subsurface PRE's			
Predicted Variable	Predictor Matrix	Entire water column	Exc. oxygen minimum layer	Oxygen minimum layer only	Exc. surface
Nitrate ( $\mu\text{mol kg}^{-1}$ )	$\theta, S_P, P$	-	0.93 (1.2)	0.77 (1.1)	-
	$\theta, S_P, P, DO$	0.96 (0.9)	-	-	-
Phosphate ( $\mu\text{mol kg}^{-1}$ )	$\theta, S_P, P$	-	0.92 (0.1)	0.77 (0.1)	-
	$\theta, S_P, P, DO$	0.94 (0.1)	-	-	-
Silicate ( $\mu\text{mol kg}^{-1}$ )	$\theta, S_P, P$	-	0.97 (0.6)	0.90 (0.6)	-
	$\theta, S_P, P, DO$	0.98 (0.6)	-	-	-
DIC ( $\mu\text{mol kg}^{-1}$ )	$\theta, S_P, P$	0.81 (11)	-	-	-
	$\theta, S_P, P, DO$	0.86 (10)	-	-	-
TA ( $\mu\text{eq kg}^{-1}$ )	$\theta, S_P, P$	-	-	-	0.59 (5)
	$\theta, S_P, P, DO$	-	-	-	0.62 (5)

**Table S1.** Summary statistics - adjusted R2 (non-brackets) and RMSE (brackets) - for sub-surface PREs (> 65 m) derived from the 2017 DY078 cruise. Two predictor matrices were used: one including dissolved oxygen and one excluding it. Different vertical extents (i.e. entire water column, excluding the surface or lower oxygen layer, or lower oxygen layer only) were used to derive the PREs for different parameters, with different vertical extents also chosen depending on the predictor matrix. For more information see section 3.1.

		2018 Sub-surface PRE's			
Predicted Variable	Predictor Matrix	Entire water column	Exc. oxygen minimum layer	Oxygen minimum layer only	Exc. surface
Nitrate ( $\mu\text{mol kg}^{-1}$ )	$\theta, S_p, P$	-	0.94 (1.2)	0.71 (1.0)	-
	$\theta, S_p, P, DO$	0.96 (1.0)	-	-	-
Phosphate ( $\mu\text{mol kg}^{-1}$ )	$\theta, S_p, P$	-	0.93 (0.1)	0.69 (0.1)	-
	$\theta, S_p, P, DO$	0.95 (0.1)	-	-	-
Silicate ( $\mu\text{mol kg}^{-1}$ )	$\theta, S_p, P$	-	0.97 (0.7)	0.60 (1.0)	-
	$\theta, S_p, P, DO$	0.97 (0.7)	-	-	-
DIC ( $\mu\text{mol kg}^{-1}$ )	$\theta, S_p, P$	0.81 (11)	-	-	-
	$\theta, S_p, P, DO$	0.93 (8)	-	-	-
TA ( $\mu\text{eq kg}^{-1}$ )	$\theta, S_p, P$	-	-	-	0.67 (5)
	$\theta, S_p, P, DO$	-	-	-	0.66 (5)

**Table S2.** Summary statistics - adjusted R2 (non-brackets) and RMSE (brackets) - for sub-surface PREs (> 65 m) derived from the 2018 AR30-04 cruise. Two predictor matrices were used: one including dissolved oxygen and one excluding it. Different vertical extents (i.e. entire water column, excluding the surface or lower oxygen layer, or lower oxygen layer only) were used to derive the PREs for different parameters, with different vertical extents also chosen depending on the predictor matrix. For more information see section 3.1.

		2020 Sub-surface PRE's			
Predicted Variable	Predictor Matrix	Entire water column	Exc. oxygen minimum layer	Oxygen minimum layer only	Exc. surface
Nitrate ( $\mu\text{mol kg}^{-1}$ )	$\theta, S_P, P$	-	0.93 (1.4)	0.70 (1.2)	-
	$\theta, S_P, P, DO$	0.96 (1.1)	-	-	-
Phosphate ( $\mu\text{mol kg}^{-1}$ )	$\theta, S_P, P$	-	0.94 (0.1)	0.68 (0.1)	-
	$\theta, S_P, P, DO$	0.95 (0.1)	-	-	-
Silicate ( $\mu\text{mol kg}^{-1}$ )	$\theta, S_P, P$	-	0.95 (0.8)	0.68 (1.0)	-
	$\theta, S_P, P, DO$	0.95 (0.8)	-	-	-
DIC ( $\mu\text{mol kg}^{-1}$ )	$\theta, S_P, P$	0.96 (6)	-	-	-
	$\theta, S_P, P, DO$	0.98 (4)	-	-	-
TA ( $\mu\text{eq kg}^{-1}$ )	$\theta, S_P, P$	-	-	-	0.65 (5)
	$\theta, S_P, P, DO$	-	-	-	0.66 (5)

**Table S3.** Summary statistics - adjusted R2 (non-brackets) and RMSE (brackets) - for sub-surface PREs (> 65 m) derived from the 2020 DY120 cruise. The October 2020 cruise was heavily impacted by covid restrictions with only around one tenth of the normal number of nutrient samples being collected. To avoid errors association with this low nutrient sample number, the '2020' PRE was generated using the 2018 and 2020 data combined. For DIC and TA, we used the 2020 data only to create the '2020' PRE. Two predictor matrices were used: one including dissolved oxygen and one excluding it. Different vertical extents (i.e. entire water column, excluding the surface or lower oxygen layer, or lower oxygen layer only) were used to derive the PREs for different parameters, with different vertical extents also chosen depending on the predictor matrix. For more information see section 3.1.

		2017-2020 Subsurface PRE's			
Predicted Variable	Predictor Matrix	Entire water column	Exc. oxygen minimum layer	Oxygen minimum layer only	Exc. surface
Nitrate ( $\mu\text{mol kg}^{-1}$ )	$\theta, S_P, P$	-	0.90 (1.6)	0.74 (1.2)	-
	$\theta, S_P, P, DO$	0.95 (1.1)	-	-	-
Phosphate ( $\mu\text{mol kg}^{-1}$ )	$\theta, S_P, P$	-	0.90 (0.1)	0.75 (0.1)	-
	$\theta, S_P, P, DO$	0.94 (0.1)	-	-	-
Silicate ( $\mu\text{mol kg}^{-1}$ )	$\theta, S_P, P$	-	0.96 (0.9)	0.90 (0.6)	-
	$\theta, S_P, P, DO$	0.96 (0.7)	-	-	-
DIC ( $\mu\text{mol kg}^{-1}$ )	$\theta, S_P, P$	0.76 (13)	-	-	-
	$\theta, S_P, P, DO$	0.87 (9)	-	-	-
TA ( $\mu\text{eq kg}^{-1}$ )	$\theta, S_P, P$	-	-	-	0.42 (7)
	$\theta, S_P, P, DO$	-	-	-	0.79 (8)

**Table S4.** Summary statistics - adjusted R2 (non-brackets) and RMSE (brackets) - for sub-surface PREs (> 65 m) derived using combined data from the 2017, 2018 and 2020 cruises. This shows that adjusted R2 values and RMSEs are comparable to when deriving PREs from single hydrographic sections (Tables S1-3). Two predictor matrices were used: one including dissolved oxygen and one excluding it. Different vertical extents (i.e. entire water column, excluding the surface or lower oxygen layer, or lower oxygen layer only) were used to derive the PREs for different parameters, with different vertical extents also chosen depending on the predictor matrix. For more information see section 3.1.

<b>Predicted Variable</b>	<b>Predictor Matrix</b>	<b>Surface PREs</b>
<b>Nitrate</b> ( $\mu\text{mol kg}^{-1}$ )	$\theta, S_P, P$	0.87 (0.9)
	$\theta, S_P, P, DO$	0.88 (0.8)
<b>Phosphate</b> ( $\mu\text{mol kg}^{-1}$ )	$\theta, S_P, P$	-
	$\theta, S_P, P, DO$	-
<b>Silicate</b> ( $\mu\text{mol kg}^{-1}$ )	$\theta, S_P, P$	0.78 (0.6)
	$\theta, S_P, P, DO$	0.78 (0.6)
<b>DIC</b> ( $\mu\text{mol kg}^{-1}$ )	$\theta, S_P, P$	-
	$\theta, S_P, P, DO$	-
<b>TA</b> ( $\mu\text{eq kg}^{-1}$ )	$\theta, S_P, P$	0.03 (8)
	$\theta, S_P, P, DO$	0.11 (8)

**Table S5.** Summary statistics - adjusted R2 (non-brackets) and RMSE (brackets) - for surface PREs (< 70 m) derived from the 2017-2018 moored water sampler deployment. Two predictor matrices were used, one including dissolved oxygen and one excluding it. No PREs exist for DIC and phosphate because of contamination of samples from the moored water sampler. Instead DIC was calculated using the derived TA record and measured pH record from the moored pH sensor, whilst the interior PRE was used for phosphate. For more information, see section 3.2.

	Error associated with:		
	Carbon / nutrient concentrations	Volume transport	Total Error
<b>Q<sub>NO3</sub> (kmol s<sup>-1</sup>)</b>	6.46	5.69	9.13
<b>Q<sub>PO4</sub> (kmol s<sup>-1</sup>)</b>	0.48	0.40	0.66
<b>Q<sub>SiO3</sub> (kmol s<sup>-1</sup>)</b>	2.44	2.41	3.65
<b>Q<sub>DIC</sub> (kmol s<sup>-1</sup>)</b>	1136	934	1550
<b>Q<sub>TA</sub> (keq s<sup>-1</sup>)</b>	1355	1065	1815

**Table S6.** Errors associated with calculating the biogeochemical transports. Two sources of error were considered: that arising from deriving the carbon and nutrient concentrations, and that arising from calculating the volume transports. The total errors, the combination of the two sources, are shown in the final column.